

CONSTITUTIVE MODELS FOR A POLY(e-CAPROLACTONE) SCAFFOLD

T.P Quinn, T.L. Oreskovic, C.N. McCowan, and N. R. Washburn

National Institute of Standards and Technology
Boulder, CO 80305

ABSTRACT

We investigate material models for a porous, polymeric scaffold used for bone. The material was made by co-extruding poly(e-caprolactone) (PCL), a biodegradable polyester, and poly(ethylene oxide) (PEO). The water soluble PEO was removed resulting in a porous scaffold. The stress-strain curve in compression was fit with a phenomenological model in hyperbolic form. This material model will be useful for designers for quasi-static analysis as it provides a simple form that can easily be used in finite element models. The ASTM D-1621 standard recommends using a secant modulus based on 10 % strain. The resulting modulus has a smaller scatter in its value compared to the coefficients of the hyperbolic model, and it is therefore easier to compare material processing differences and ensure quality of the scaffold. A third material model was constructed from images of the microstructure. Each pixel of the micrographs was represented with a brick finite element and assigned the Young's modulus of bulk PCL or a value of 0 for a pore. A compressive strain was imposed on the model and the resulting stresses were calculated. The elastic constants of the scaffold were then computed using Hooke's law for a linear-elastic isotropic material. The model was able to predict the small strain Young's modulus measured in the experiments to within one standard deviation. Thus, by knowing the microstructure of the scaffold, its bulk properties can be predicted from the material properties of the constituents.

Keywords: tissue engineering, scaffold, PCL, mechanical properties, stress-strain curve, finite element model, secant modulus, hyperbolic model

1 INTRODUCTION

This work presents empirical and theoretical models of the mechanical response of a porous (e-caprolactone) (PCL) scaffold to a quasi-statically applied stress. One possible method to replace injured or missing bone is by using a biodegradable, synthetic scaffold that can be shaped into the proper geometry before insertion into the body. The scaffold can be cultured with cells *in vitro*, or a bare (or initially seeded) scaffold can be used. In both cases the mechanical properties of the scaffold or scaffold/tissue construct must be known in order to ensure that it does not fail mechanically after it is implanted. A typical approach would be for the implant designer to use a finite element model to predict the response of the implant to *in vivo* loads. The mechanical quality of the scaffolds must be assured before they are implanted as well. Here, we present methodology for developing empirical and theoretical material models to address the need for quality assurance, and we demonstrate them using a PCL scaffold as an example.

The mechanical properties of candidate scaffold materials have been measured but usually only the modulus and strength of the material are reported (for examples see [1-4]). Zein et al. [5] found a good correlation between the yield strength, yield strain, and initial modulus in compression with the porosity of variously structured PCL scaffolds. Ma and Zang [6] reported the initial modulus and yield strength in compression of poly(L-lactic acid) and poly(D,L-lactic acid-co-glycolic acid) scaffolds as a function of polymer concentration. These synthetic polymers usually exhibit a nonlinear stress-strain curve that is not easily represented by the initial linear region, however.

In this research, a model form of the stress-strain response of the material in compression has been developed. The model can easily be used for finite element calculations of the response of an implant made of the scaffold material. We compare the parameters of our model to the secant modulus that is recommended for rigid cellular plastics by ASTM [7]. Finally we present a method for prediction of the initial modulus based on the microstructure of the scaffold material.

2 MATERIALS AND METHODS

Scaffold Fabrication

The PCL scaffold we used was originally a coextrusion of PCL and poly(ethylene oxide) (PEO) and is described fully in [8]. The PEO is water soluble and can be washed out of the PCL leaving a network of interconnected pores. The pore structure can be modified by annealing the blend for different amounts of time. PCL has been shown to be biocompatible with different cell types [1, 8].

In brief, the polymers were blended using a twin screw minicomponenter and extruded tubes of polymer were cut into 4 mm cylindrical pieces and annealed in a vacuum oven at 80 °C. The copolymer was then molded into square bars 5 x 5 x ~25 mm and allowed to anneal at 100 °C for 15, 30 and 60 minutes. The rods were cut into 5 x 5 x 5 mm cubes from which the final 3 x 3 x 3 mm samples were machined. Care was taken so that the final samples came from the center of the 5 mm cubes. At least six specimens were made for the three different anneal times. The samples were weighed dry and then suspended in distilled water on a shaker table for 24 - 48 hours to remove the water soluble PEO. Samples were then dried in a dessicator and weighed again. Porosity resulted in the range of 47 % - 58 % (by weight) for all samples. Samples were resuspended in water for 24 hours before compression testing.

Mechanical Testing

A table-top, servo-hydraulic, materials-testing machine of 5000 N capacity outfitted with 20 mm diameter platens was used for compression testing. The compression of one face of the sample was recorded with a video microscope with a resolution of about 6 μm per pixel. The load was measured with a ±100 N load cell with an absolute error of less than 0.1 % .

The samples were tested in displacement control with the crosshead velocity set to 3×10^{-3} mm/s for a nominal strain rate of 1×10^{-3} s⁻¹. The average strain in the sample was calculated using image correlation of the video. The image correlation was done by selecting a region of 384 x 288 pixels in the center of the specimen. The region was then subdivided in 32 x 32 pixel subimages as in [9]. A displacement vector was estimated for each subimage by maximizing the correlation between the base image (see Figure 1) and the deformed image using bi-cubic splines to interpolate between pixels. Lines

were then fitted to each column (or row) of squares that were vertically (or horizontally) adjacent. Assuming that the strain was uniform, the slopes of these lines were averaged to estimate the normal strains in the sample. To keep the displacements to a few pixels or less, the base image was updated every tenth frame or 21 s. The absolute displacement was maintained by adding the displacement of subsequent frames to the displacements that were already calculated for the new base image.

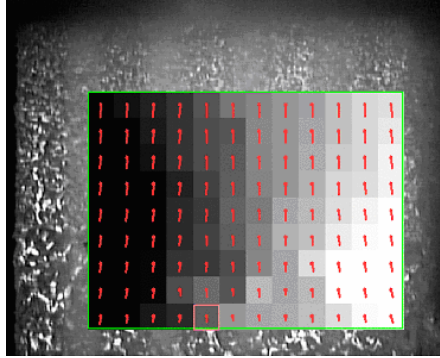


Figure 1: The displacement vectors superimposed on the subimages.

The resulting stress-strain (σ - ε) curve was fitted with a phenomenological model in hyperbolic form: $\sigma = E \frac{\varepsilon}{1 + A\varepsilon}$, where the fitted parameter E is the modulus of the material at small strains, and the fitted parameter A is the (dimensionless) strain coefficient. The model asymptotically approaches $\sigma = E/A$ for large strains. For large A , the material approaches an elastic-perfectly plastic state; for small A , the material does not exhibit a linear-elastic region. The secant modulus was also calculated according to [7]. For this material, the secant modulus can be taken as ten times the stress at 10 % strain.

The data are expressed as means with standard deviations. A three-way comparison of an analysis of variance (ANOVA) was used to assess the statistical significance.

Optical coherence microscopy (OCM) [10] was used to scan the interior of the scaffold samples. Each image of 250 x 250 pixels covers 1 mm² (920 μm^2) with a depth of 4 μm per slice. Five image slices from two scaffold samples from each of the anneal groups were examined using OCM. The grey scale OCM images were converted to a binary image by use of a threshold after despeckling, and the area of the pores were measured automatically with image analysis software. Average pore size areas were calculated by averaging the ten slices for each anneal group.

Modulus Prediction

Finally, a finite element (FE) model was constructed to predict the elastic constants of the material at small strains given the microstructure. The 4 μm cubic pixels from the OCM analysis were used to identify the pores in the material. Each pixel was represented with a brick element and assigned the Young's modulus of bulk PCL, and a value of 0 for a pore. A compressive strain was imposed on the model and the resulting stresses were calculated. The elastic constants of scaffold were then calculated using Hooke's law for a linear-elastic, isotropic material.

3 RESULTS

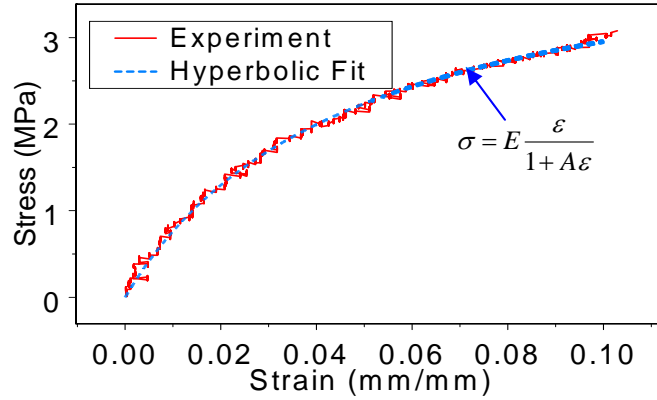


Figure 2: The stress-strain curve in compression for a PCL scaffold with pore size area of 0.0150 mm².

The PCL samples show a nonlinear response to the applied stress (Figure 2). The hyperbolic fit was able to approximate the data well, as seen in Figure 2. The results of the modeling and pore size analysis for the three different pore sizes are summarized in Table 1. PCL scaffolds showed smaller mean values of E and A at the pore size of 0.0014 mm² than for the other two pore sizes (Figure 3 and Table 1), but these differences were not significant. The secant modulus also increases from 0.0014 mm² to the other two pore sizes, and the difference is significant.

Table 1. Summary of results of model parameters and pore size.

Pore Size Area (mm ²)	E (MPa)	A	Secant Modulus (MPa)
0.0014	89 ± 40	19 ± 10	30 ± 5*
0.0039	122 ± 60	21 ± 13	38 ± 6
0.0150	144 ± 58	31 ± 18	36 ± 5

* Significantly different $p < 0.05$ from the secant modulus of the other two pore size samples. No other parameters showed significance.

The FE model was constructed based on the microstructure of samples with a mean pore size of 0.0150 mm² (Figure 4). The FE model predicted an E of 87 ± 41 MPa, which is within one standard deviation of the E for a pore size of 0.015 mm².

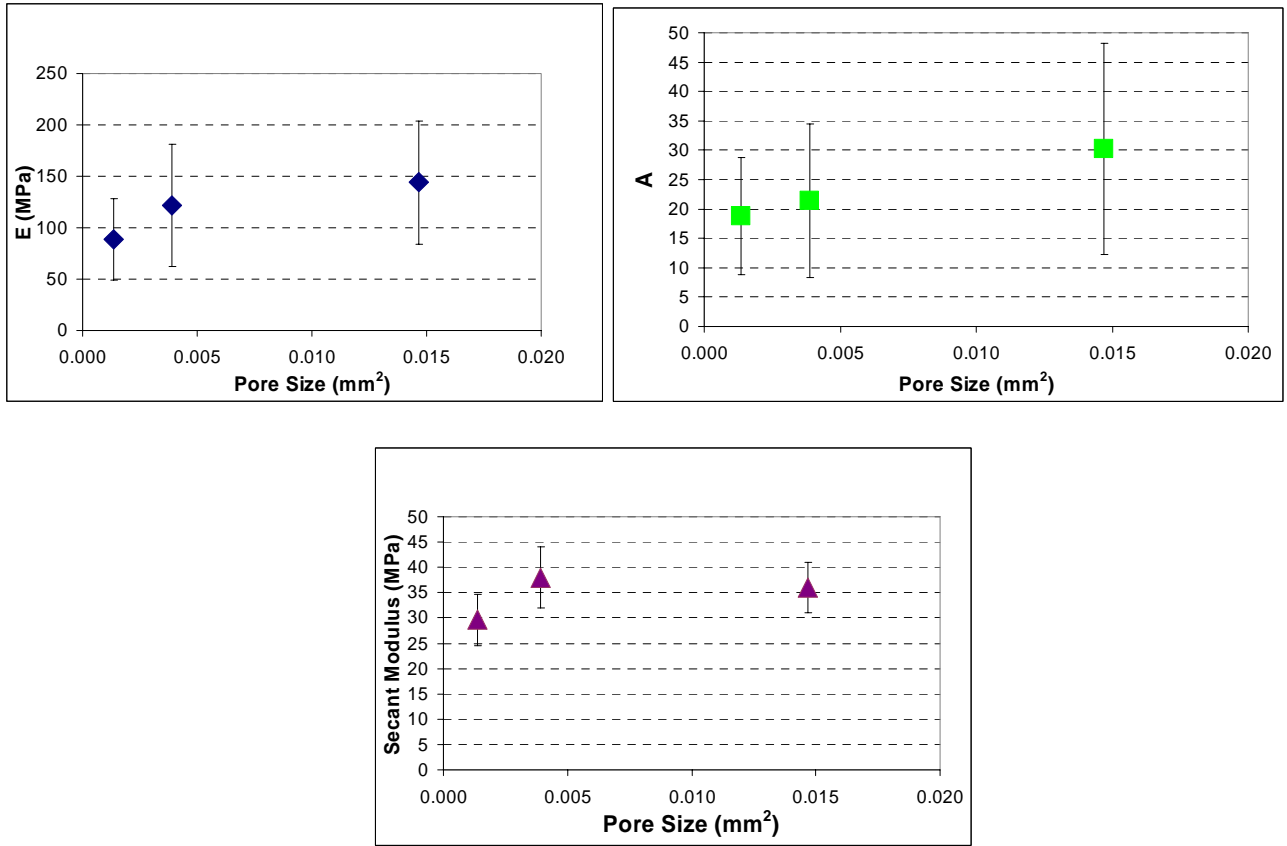


Figure 3: The model parameters and secant modulus as a function of pore size.

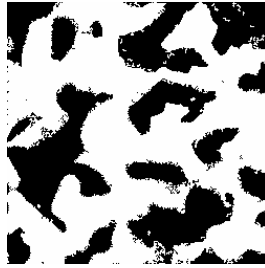


Figure 4: The material map for the finite element model of the porous PCL scaffold. Black indicates a pore.

4 DISCUSSION

It is clear from Figure 2 that the PCL cannot easily be approximated linearly up to 10 % strain. This hyperbolic material model will therefore be useful for designers of implants made with these types of materials for quasi-static analysis, as it provides a simple form that can easily be used in FE models. The hyperbolic model has the drawback of having relatively large standard deviations in its fitted parameters E and A (up to 49 % of the mean for E and up to 61 % of the mean for A). That is because this material's variability in its stress-strain curve up to 10 % strain. The secant modulus offers a much

lower variability with the standard deviation, at most 16 % of the mean. It is most likely this reduced variability and ease of computation that led to its adoption in the standard [7]. These traits make the secant modulus ideal for use in quality control of scaffold materials. It is likely that as the pore size increases (while maintaining the volume fraction of pores in the material), the secant modulus increases but then levels off. More data at small pore sizes must be collected to confirm this hypothesis, however.

The result from the FE model indicates that it is possible to predict the properties of the scaffold at least roughly from knowledge of the microstructure of the scaffold and the bulk material properties.

5 SUMMARY

Material models fit to the compressive stress-strain curve for a PCL scaffold material were constructed. A hyperbolic model fitted the data well to 10 % strain. Relatively large standard deviations in the model parameters compared to the means were evident. A secant modulus was also measured and found to have less variability and therefore making it useful for quality control purposes. Finally the initial modulus of the material was roughly predicted from the microstructure and the bulk material properties.

6 REFERENCES

- [1] D. W. Hutmacher, T. Schantz, I. Zein, K. W. Ng, S. H. Teoh, and K. C. Tan, "Mechanical properties and cell cultural response of polycaprolactone scaffolds designed and fabricated via fused deposition modeling," *J Biomed Mater Res*, vol. 55, pp. 203-16, 2001.
- [2] I. Engelberg and J. Kohn, "Physico-mechanical properties of degradable polymers used in medical applications: a comparative study," *Biomaterials*, vol. 12, pp. 292-304, 1991.
- [3] T. M. Chu, D. G. Orton, S. J. Hollister, S. E. Feinberg, and J. W. Halloran, "Mechanical and in vivo performance of hydroxyapatite implants with controlled architectures," *Biomaterials*, vol. 23, pp. 1283-93, 2002.
- [4] Y. Zhang and M. Zhang, "Three-dimensional macroporous calcium phosphate bioceramics with nested chitosan sponges for load-bearing bone implants," *J Biomed Mater Res*, vol. 61, pp. 1-8, 2002.
- [5] I. Zein, D. W. Hutmacher, K. C. Tan, and S. H. Teoh, "Fused deposition modeling of novel scaffold architectures for tissue engineering applications," *Biomaterials*, vol. 23, pp. 1169-85, 2002.
- [6] P. X. Ma and R. Zhang, "Microtubular architecture of biodegradable polymer scaffolds," *J Biomed Mater Res*, vol. 56, pp. 469-77, 2001.
- [7] ASTM, "Standard test method for compressive properties of rigid cellular plastics," D 1621 - 00, 2000.
- [8] N. R. Washburn, C. G. Simon, Jr., A. Tona, H. M. Elgendy, A. Karim, and E. J. Amis, "Co-extrusion of biocompatible polymers for scaffolds with co-continuous morphology," *J Biomed Mater Res*, vol. 60, pp. 20-9, 2002.
- [9] D. T. Read and Y.-W. Cheng, "Proposed standardization effort: digital-image correlation for mechanical testing," presented at SEM Annual Conference on Experimental and Applied Mechanics, Portland, OR, 2001.
- [10] J. D. Dunkers, M. T. Cicerone, and N. R. Washburn, "Collinear optical coherence and confocal fluorescence microscopies for tissue engineering," *Optics Express*, vol. 11, pp. 3074-79, 2003.